

# Width bifurcation and dynamical phase transitions in open quantum systems

Hichem Eleuch<sup>1,2,\*</sup> and Ingrid Rotter<sup>3,\*\*</sup>

<sup>1</sup>*Ecole Polytechnique, C.P. 6079, succ. Centre ville, Montréal (QC), Canada H3C 3A7*

<sup>2</sup>*Université de Montréal, C.P. 6128, Succ. Centre-Ville,  
Montréal (QC), H3C 3J7 Canada and*

<sup>3</sup>*Max Planck Institute for the Physics of Complex Systems, D-01187 Dresden, Germany*

(Dated: August 21, 2018)

## Abstract

The states of an open quantum system are coupled via the environment of scattering wavefunctions. The complex coupling coefficients  $\omega$  between system and environment arise from the principal value integral and the residuum. At high level density where the resonance states overlap, the dynamics of the system is determined by exceptional points. At these points, the eigenvalues of two states are equal and the corresponding eigenfunctions are linearly dependent. It is shown in the present paper that  $\text{Im}(\omega)$  and  $\text{Re}(\omega)$  influence the system properties differently in the surrounding of exceptional points. Controlling the system by a parameter, the eigenvalues avoid crossing in energy near an exceptional point under the influence of  $\text{Re}(\omega)$  in a similar manner as it is well known from discrete states.  $\text{Im}(\omega)$  however leads to width bifurcation and finally (when the system is coupled to one channel, i.e. to a common continuum of scattering wavefunctions), to a splitting of the system into two parts with different characteristic time scales. Physically, the system is stabilized by this splitting since the lifetimes of most  $(N - 1)$  states are longer than before while that of only one state is shorter. In the cross section the short-lived state appears as a background term in high-resolution experiments. The wavefunctions of the long-lived states are mixed in those of the original ones in a comparably large parameter range. Numerical results for the eigenvalues and eigenfunctions are shown for  $N = 2, 4$  and 10 states coupled mostly to 1 channel.

## I. INTRODUCTION

The description of quantum mechanical systems by means of the Schrödinger equation has been developed more than 80 years ago. At that time only a few resonance states in nuclei and atoms were known which are well separated from one another. The energies of these states are well described by means of the Schrödinger equation with a Hermitian Hamiltonian. In order to describe the finite lifetimes of these states, the R-matrix theory has been developed which is however too complicated for practical calculations. The finite lifetimes of the individual states are calculated usually perturbatively, see e.g. [1]. Later, systems at high level density were in the center of interest. Under these conditions, a statistical description of the system turned out to be very efficient [2]. The resonances are well isolated from one another, and the lifetimes of the states are very long and do not play any role.

In the course of time, experimental studies have been performed for different quantum systems with a much improved accuracy. Also the theoretical calculations are carried out today not only for states being well separated in energy from one another but also for resonance states in the regime of overlapping. Here the single individual states can no longer be identified what results in problems of their interpretation. Contradictions between experimental results and conventional Hermitian quantum physics appeared in different small quantum systems. For example, Heiblum et al. [3] found experimentally a crossover from the mesoscopic to a universal phase for electron transmission in quantum dots about than 10 years ago. These results could not be explained in conventional quantum physics in spite of much effort [4]. Recently Koehler et al. [5] observed that neutron resonance data exclude random matrix theory. Deviations between experimental data and random matrix theory in nuclear physics studies were observed also earlier, e.g. [6]. These and other experimental results show that the Schrödinger equation originally introduced with a Hermitian Hamilton operator for the description of well isolated resonances, has to be extended. Above all, the lifetimes of the resonance states have to be calculated also in the regime of overlapping resonances and the justification of statistical assumptions has to be proven for small quantum systems.

The lifetimes of the resonance states can be calculated when the system is explicitly considered to be open and the calculations are performed quantum mechanically for both the

system and the environment of scattering wavefunctions into which the system is embedded. Using the Feshbach projection operator technique [7], first the *energy-independent* many-body problem of the system (with the Hermitian Hamiltonian  $H_B$ ) is solved in the standard manner. These solutions provide the energies  $E_i^B$  and wavefunctions  $\Phi_i^B$  of the discrete states with inclusion of the so-called *internal* interaction. In a second step, the *energy-dependent* scattering wavefunctions  $\xi_c^E$  of the environment are calculated and, further, the (energy-dependent) coupling matrix elements

$$\gamma_{kc}^0 = \sqrt{2\pi} \langle \Phi_k^B | V | \xi_c^E \rangle . \quad (1)$$

between the discrete states of the system and the environment are evaluated (see [8], section 2.1). The corresponding Schrödinger equation contains an energy dependent (nonlinear) source term describing the coupling between system and environment. The Hamiltonian  $\mathcal{H}_0$  of this equation is non-Hermitian and provides the lifetimes of the states, but without any additional interaction of the states via the environment. The Schrödinger equation with  $\mathcal{H}_0$  and source term can be rewritten into a Schrödinger equation without source term but with a non-Hermitian Hamiltonian  $\mathcal{H}$  that contains the interaction of the states via the environment (the so-called *external* interaction) in the nondiagonal matrix elements [9]. The Hamiltonian  $\mathcal{H}$  reads

$$\mathcal{H} = H_B + V_{BC} G_C^{(+)} V_{CB} \quad (2)$$

where  $V_{BC}$  and  $V_{CB}$  stand for the coupling between system and environment and  $G_C^{(+)}$  is the Green function in the subspace of scattering states. The external interaction of the states via the continuum is complex, generally. The principal value integral is

$$\text{Re} \langle \Phi_i^B | \mathcal{H} | \Phi_j^B \rangle - E_i^B \delta_{ij} = \frac{1}{2\pi} \sum_{c=1}^C \mathcal{P} \int_{\epsilon_c}^{\epsilon'_c} dE' \frac{\gamma_{ic}^0 \gamma_{jc}^0}{E - E'} \quad (3)$$

and the residuum reads

$$\text{Im} \langle \Phi_i^B | \mathcal{H} | \Phi_j^B \rangle = -\frac{1}{2} \sum_{c=1}^C \gamma_{ic}^0 \gamma_{jc}^0 . \quad (4)$$

The interaction of the states of the system via the environment is involved in the eigenvalues  $\mathcal{E}_i$  and eigenfunctions  $\Phi_i$  of the Hamiltonian  $\mathcal{H}$ . It is therefore relatively easy, in this formalism, to study the influence of the environment onto the states of the system. That means, the non-Hermitian quantum physics is – in contrast to the widely spread meaning

– *not* a further approximation introduced in the theory. It is an expression of the fact that the system considered is really open and its properties are influenced by the coupling to the environment. This influence is unimportant at low level density where it can be described by perturbation theory. It becomes, however, decisive in the regime of overlapping resonances.

Meanwhile, many calculations for open quantum systems are performed with high accuracy. Without using any perturbation theory or statistical assumptions, the Schrödinger equation with the non-Hermitian Hamilton operator  $\mathcal{H}$  is solved and the eigenvalues  $\mathcal{E}_i = E_i - \frac{i}{2}\Gamma_i$  and eigenfunctions  $\Phi_i$  are obtained. That means, not only the energies  $E_i$  of the states of the system are evaluated but also their lifetimes  $\tau_i \propto 1/\Gamma_i$ . The control of the eigenvalues by a parameter allows to draw conclusions on the dynamics of open quantum systems.

The limits of the applicability of the standard quantum theory with Hermitian Hamilton operator can be seen best at high level density, where the individual resonance states overlap and interact with one another via the continuum of scattering wavefunctions. Here, the dynamics of the system is determined by singular points, the so-called *exceptional points*. They cause level repulsion in energy as well as a bifurcation of the widths (inverse proportional to the lifetimes) of the states. Results are obtained theoretically as well as experimentally, which are counterintuitive at first glance: due to width bifurcation, coherent short-lived states are formed together with states that are almost decoupled from the continuum of scattering states [8, 10, 11]. An example is the above-mentioned crossover from the mesoscopic to a universal phase in the transmission in quantum dots [3] and its qualitative explanation on the basis of a Schrödinger equation with non-Hermitian Hamilton operator [12]. This phenomenon is observed in different systems and is called usually *dynamical phase transition* [13]. The short-lived states are analog to the coherent superradiant states considered by Dicke [14] in 1954 as shown by means of a toy model [15]. Moreover, it could be shown in an experiment on non-locally coupled pairs of quantum point contacts that discrete states undergo a robust interaction that is achieved by coupling them to each other through the continuum [16]. Most of these results are of high value for fundamental questions of quantum mechanics as well as for applications.

It is the aim of the present paper to show some generic (mostly numerical) results for open quantum systems in order to receive a deeper understanding for the dynamical phase transitions occurring in the regime of overlapping resonances. A toy model is used in order

to receive conclusions on the role played by exceptional points and avoided level crossings at high level density in open quantum systems. Of special interest are the effects arising from the imaginary part (4) of the coupling term via the environment.

The calculations are performed with respectively two, four and ten resonance states coupled mostly to one open decay channel (corresponding to the common continuum of scattering wavefunctions) under the condition that they avoid crossing or even cross in a certain parameter range. The coupling of  $N$  resonance states to  $K < N$  channels corresponds to the general situation of open quantum systems. The formalism used in the calculations is the same as that discussed in our earlier paper [17]. The results show very clearly that the imaginary part of the coupling term between system and environment causes width bifurcation and, finally, the formation of different time scales in the regime of overlapping resonances. Due to width bifurcation, the system splits into two parts that exist at different times. This process is irreversible. The wavefunctions of the short-lived *aligned* states are mixed coherently in relation to the open decay channel while those of the long-lived *trapped* states are mixed incoherently such that the states are almost decoupled from the open decay channel.

The results confirm the characteristic features of the dynamical phase transitions appearing in open quantum systems at high level density. They show that the number of states of the system is reduced during the dynamical phase transition due to ejecting the aligned short-lived state and, furthermore, that the wavefunctions of the states before and beyond the dynamical phase transition are completely different from one another. While the states of the original system (without interaction via the continuum) have individual spectroscopic features, those of the system consisting of the long-lived states beyond the dynamical phase transition show chaotic features. These results prove once more that the experimental results [3] on the crossover from the mesoscopic to a universal phase for electron transmission in quantum dots can be explained by means of the non-Hermiticity of the Hamiltonian. Additionally it should be mentioned here that the aligned state corresponds to the Dicke superradiant state and the trapped states to the subradiant states which are considered in optics, e.g. [18].

In section II, we sketch the formalism used in the present calculations. For  $N = 2$  states with equal decay widths, the analytical and numerical solutions of the problem show clearly the effect of width bifurcation. Numerical results for eigenvalues and eigenfunctions

obtained for  $N = 2, 4$  and 10 states are provided in sections III to VI. The results are discussed in section VII while conclusions on the relation between exceptional points and width bifurcation are drawn in the last section VIII.

## II. FORMALISM

We consider an  $N \times N$  matrix

$$\mathcal{H} = \begin{pmatrix} \epsilon_1 + \omega_{11} & \omega_{12} & \dots & \omega_{1N} \\ \omega_{21} & \epsilon_2 + \omega_{22} & \dots & \omega_{2N} \\ \vdots & \vdots & \ddots & \vdots \\ \omega_{N1} & \omega_{N2} & \dots & \epsilon_N + \omega_{NN} \end{pmatrix} \quad (5)$$

the diagonal elements of which are the  $N$  complex eigenvalues  $\epsilon_i + \omega_{ii} \equiv e_i - i/2 \gamma_i$  of a non-Hermitian operator. The  $\omega_{ii}$  are the so-called selfenergies of the states arising from their coupling to the environment of scattering wavefunctions into which the system is embedded. In atomic physics, these values are known as Lamb shift. Our calculations are performed with coupling matrix elements  $\omega_{ii}$  the values of which do not depend on the parameter considered. In such a case, the  $\omega_{ii}$  can be considered to be included into the diagonal matrix elements, which read  $\varepsilon_i \equiv \epsilon_i + \omega_{ii}$ . The  $e_i$  and  $\gamma_i$  denote the energies and widths, respectively, of the  $N$  states (including their selfenergies) without account of the interaction of the different states via the environment.

The internal interaction of the two states  $i$  and  $k \neq i$  (appearing in the closed system) *as well as* their external interaction (via the environment) are contained in the  $\omega_{ik}$ . The internal interaction can be caused only by some part of  $\text{Re}(\omega_{ik})$  while the external interaction contains complex  $\omega_{ik}$ , see equations (3) and (4). Most interesting part of the external interaction is therefore  $\text{Im}(\omega_{ik})$ . It becomes important at high level density where the corresponding resonance states overlap.

When the number  $N$  of states is equal to the number  $K$  of common channels (i.e. equal to the number  $K$  of different common continua of scattering wavefunctions) all the coupling matrix elements  $\omega_{ik}$  are different from zero and the matrix (5) is full. In the case with only one open decay channel  $K = 1$ , all  $\omega_{ik}$  different from  $\omega_{i \ k=K}$  and  $\omega_{i=K \ k}$  are zero. An

example of  $N = 4$  states coupled to only the fourth channel is the following matrix

$$\mathcal{H} = \begin{pmatrix} \varepsilon_1 & 0 & 0 & \omega_{14} \\ 0 & \varepsilon_2 & 0 & \omega_{24} \\ 0 & 0 & \varepsilon_3 & \omega_{34} \\ \omega_{41} & \omega_{42} & \omega_{43} & \varepsilon_4 \end{pmatrix} \quad (6)$$

with  $\varepsilon_i = \epsilon_i$  for  $i \neq 4$  and  $\varepsilon_4 = \epsilon_4 + \omega_{44}$ .

The eigenvalues of  $\mathcal{H}$  will be denoted by  $\mathcal{E}_i \equiv E_i - i/2 \Gamma_i$  where  $E_i$  and  $\Gamma_i$  stand for the energy and width, respectively, of the eigenstate  $i$ . The eigenfunctions of the non-Hermitian  $\mathcal{H}$  are biorthogonal (see sections 2.2 and 2.3 of [8]),

$$\langle \Phi_i^* | \Phi_j \rangle = \delta_{ij} . \quad (7)$$

It follows

$$\langle \Phi_i | \Phi_i \rangle = \text{Re} (\langle \Phi_i | \Phi_i \rangle) ; \quad A_i \equiv \langle \Phi_i | \Phi_i \rangle \geq 1 \quad (8)$$

and

$$\begin{aligned} \langle \Phi_i | \Phi_{j \neq i} \rangle &= i \text{Im} (\langle \Phi_i | \Phi_{j \neq i} \rangle) = -\langle \Phi_{j \neq i} | \Phi_i \rangle \\ |B_i^j| &\equiv |\langle \Phi_i | \Phi_{j \neq i} \rangle| \geq 0 . \end{aligned} \quad (9)$$

At an exceptional point,  $A_i \rightarrow \infty$  and  $|B_i^j| \rightarrow \infty$ . The  $\mathcal{E}_i$  and  $\Phi_i$  contain global features that are caused by many-body forces induced by the coupling  $\omega_{ik}$  of the states  $i$  and  $k \neq i$  via the environment, see equations (3), (4) and the corresponding discussion in [11, 19].

In the case  $N = 2$ , the two eigenvalues of  $\mathcal{H}$  are

$$\mathcal{E}_{i,j} \equiv E_{i,j} - \frac{i}{2} \Gamma_{i,j} = \frac{\varepsilon_1 + \varepsilon_2}{2} \pm Z ; \quad Z \equiv \frac{1}{2} \sqrt{(\varepsilon_1 - \varepsilon_2)^2 + 4\omega^2} . \quad (10)$$

According to this expression, two interacting discrete states (with  $\gamma_k = 0$ ) avoid always crossing since  $\omega$  and  $\varepsilon_1 - \varepsilon_2$  are real in this case. Resonance states with nonvanishing widths  $\Gamma_i$  repel each other in energy according to the value of  $\text{Re}(Z)$  while the widths bifurcate according to the value of  $\text{Im}(Z)$ . The two states cross when  $Z = 0$ . This crossing point is an exceptional point according to the definition of Kato [20].

At the exceptional point  $Z = 0$ , the eigenfunctions of (5) of the two crossing states are linearly dependent from one another,

$$\Phi_1^{\text{cr}} \rightarrow \pm i \Phi_2^{\text{cr}} ; \quad \Phi_2^{\text{cr}} \rightarrow \mp i \Phi_1^{\text{cr}} \quad (11)$$

according to analytical as well as numerical and experimental studies, see Appendix of [11] and section 2.5 of [8]. That means, the wavefunction  $\Phi_1$  of the state 1 jumps, at the exceptional point, via the wavefunction  $\Phi_1 \pm i\Phi_2$  of a chiral state to  $\pm i\Phi_2$  [21]. From (11) follows:

- (i) When two levels are distant from one another, their eigenfunctions are (almost) orthogonal,  $\langle \Phi_k^* | \Phi_k \rangle \approx \langle \Phi_k | \Phi_k \rangle = A_k \approx 1$ .
- (ii) When two levels cross at the exceptional point, their eigenfunctions are linearly dependent according to (11) and  $\langle \Phi_k | \Phi_k \rangle \equiv A_k \rightarrow \infty$ .

These two relations show that the phases of the two eigenfunctions relative to one another change when the crossing point is approached. This can be expressed quantitatively by defining the *phase rigidity*  $r_k$  of the eigenfunctions  $\Phi_k$ ,

$$r_k \equiv \frac{\langle \Phi_k^* | \Phi_k \rangle}{\langle \Phi_k | \Phi_k \rangle} = A_k^{-1}. \quad (12)$$

It holds  $1 \geq r_k \geq 0$ . The non-rigidity  $r_k$  of the phases of the eigenfunctions of  $\mathcal{H}$  follows also from the fact that  $\langle \Phi_k^* | \Phi_k \rangle$  is a complex number (in difference to the norm  $\langle \Phi_k | \Phi_k \rangle$  which is a real number) such that the normalization condition (7) can be fulfilled only by the additional postulation  $\text{Im}\langle \Phi_k^* | \Phi_k \rangle = 0$  (what corresponds to a rotation).

When  $r_k < 1$ , an analytical expression for the eigenfunctions as a function of a certain control parameter can, generally, not be obtained. An exception is the special case  $\gamma_1 = \gamma_2$  for which  $Z = \frac{1}{2}\sqrt{(e_1 - e_2)^2 + 4\omega^2}$ . In this case, the condition  $Z = 0$  can not be fulfilled if  $\omega = x$  is real due to

$$(e_1 - e_2)^2 + 4x^2 > 0. \quad (13)$$

The exceptional point can be found only by analytical continuation into the continuum [8, 9] and the two states avoid crossing. This is analogue to the avoided level crossings of discrete states.

The condition  $Z = 0$  can be fulfilled however if  $\omega = ix$  is imaginary,

$$(e_1 - e_2)^2 - 4x^2 = 0 \rightarrow e_1 - e_2 = \pm 2x, \quad (14)$$

and two exceptional points appear. It holds further

$$(e_1 - e_2)^2 > 4x^2 \rightarrow Z \in \Re \quad (15)$$

$$(e_1 - e_2)^2 < 4x^2 \rightarrow Z \in \Im \quad (16)$$



independent of the parameter dependence  $e_i(a)$ . In the first case, the eigenvalues  $\mathcal{E}_i = E_i - i/2 \Gamma_i$  differ from the original values  $\varepsilon_i = e_i - i/2 \gamma_i$  by a contribution to the energies and in the second case by a contribution to the widths. The width bifurcation starts at one of the exceptional points and becomes maximum in the middle between the two exceptional points. This happens at the crossing point  $e_1 = e_2$  where  $\Delta\Gamma/2 \equiv |\Gamma_1/2 - \Gamma_2/2| = 4x$ .

Some years ago, the case  $N = 2$  with  $e_i = e_i(a)$ , fixed real  $\omega \equiv \omega_{12} = \omega_{21}$ , and different fixed values of  $\gamma_i$ , including  $\gamma_i = 0$ , is studied as a function of the parameter  $a$  in the neighborhood of avoided and true crossings of the two levels [9]. The results for the  $N = 2$  case [9] show further that the wavefunctions of the two states  $\Phi_1$  and  $\Phi_2$  are mixed in a finite range of the parameter  $a$  around the critical value  $a_{\text{cr}}$  at which the two states avoid crossing. This holds true not only for resonance states but also for discrete states.

The eigenfunctions  $\Phi_i$  of  $\mathcal{H}$  can be represented in the set of basic wavefunctions  $\phi_i$  of the unperturbed matrix (corresponding to the case with vanishing coupling matrix elements  $\omega_{ij}$ ),

$$\Phi_i = \sum_{j=1}^N b_{ij} \phi_j . \quad (17)$$

Also the  $b_{ij}$  are normalized according to the biorthogonality relations of the wavefunctions  $\{\Phi_i\}$ .

In our calculations, the mixing coefficients  $b_{ij}$  of the wavefunctions of the two states due to their avoided crossing are not calculated. We simulate the fact that the two wavefunctions are mixed in a finite parameter range around the critical value of their avoid crossing [9] by assuming a Gaussian distribution

$$\omega_{i \neq j} = \omega e^{-(e_i - e_j)^2} \quad (18)$$

for the coupling coefficients. The results reproduce very well those discussed in [9] for 2 levels and real coupling  $\omega$ .

Of special interest is the situation at high level density where the ranges of avoided crossings, defined by (18), of different levels overlap. Some generic results obtained with 2, 4 and 10 resonance states will be presented in the following sections.

### III. EIGENVALUES AND EIGENFUNCTIONS FOR $N = 2$ CROSSING LEVELS

We start our calculations with the two-level case which is studied mostly in literature. We choose the matrix (5) with  $e_i = e_i(a)$ , different fixed values of  $\gamma_i$  and fixed  $\omega$ . The functional dependence of the energies over the parameter  $a$  is similar as in [9, 17]. However, the  $\omega$  are real in [9] while they are mostly complex in the present paper as well as in [17]. According to (10) to (16), the exceptional points appear at different values of the parameter  $a$  when the ratio  $\text{Re}(\omega)$  to  $\text{Im}(\omega)$  is varied, see also Figs. 1 to 3 in [17].

In Fig. 1 we show the numerical results for the avoided level crossing phenomenon as a function of the parameter  $a$  beyond, at and below the exceptional point. In all cases, the value of  $\omega$  is fixed to  $0.05(1+i)$  while the  $\gamma_1/2$  are different in the different subfigures (with  $\gamma_2/\gamma_1 = 1.1$  in all cases). The exceptional point appears at  $\gamma_1^{\text{cr}}/2 = 1$ , see Figs. 1. c, d. When  $\gamma_1/2 > \gamma_1^{\text{cr}}/2$  (Figs. 1. a, b), the eigenvalue trajectories cross in energy while the widths  $\Gamma_1$  and  $\Gamma_2$  are always different from one another. The situation is another one when  $\gamma_1/2 < \gamma_1^{\text{cr}}/2$ . Here, the eigenvalue trajectories avoid crossing in energy while the trajectories  $\Gamma_1$  and  $\Gamma_2$  cross at certain values of  $a$  (Figs. 1. e to h).

The comparison of Fig. 1 with complex  $\omega = 0.05(1+i)$  and Fig. 2 in [9] with real  $\omega = 0.05$  shows the influence of  $\text{Im}(\omega)$ . While the  $\Gamma_i(a)$  vary symmetrically around the critical value  $a^{\text{cr}}$  when  $\omega$  is real, this is not the case when  $\omega$  is complex. In the last case, the difference  $\Gamma_1 - \Gamma_2$  blows up in the critical region. Furthermore, the  $\Gamma_i$  approach their asymptotic values in a relatively small parameter range of  $a$  when  $\omega$  is real in contrast to the case with complex  $\omega$ . These results will be discussed further in the following sections.

In Fig. 2, we show the mixing coefficients  $|b_{ij}|^2$  of the eigenfunctions as a function of the parameter  $a$  corresponding to the eigenvalue figures shown in Fig. 1. The mixing coefficient is complex,  $\omega = 0.05(1+i)$ . This figure can be compared with Fig. 5 in [9] calculated exactly with real  $\omega = 0.05$ . In both cases, the difference between the two curves  $|b_{ij}|^2$  is always 1 when  $\gamma_1/2 > \gamma_1^{\text{cr}}/2$ . This result corresponds to the fact that the two states will not be exchanged when  $\gamma_1/2 > \gamma_1^{\text{cr}}/2$ . The energy trajectories of the eigenstates cross freely and the widths of the two states are always different from one another, see Figs. 1. a, b.

At the exceptional point (where  $\gamma_1/2 = \gamma_1^{\text{cr}}/2$ ),  $|b_{ij}|^2 \rightarrow \infty$  in both cases. When  $\gamma_1/2 < \gamma_1^{\text{cr}}/2$ , the two curves  $|b_{ij}|^2$  coincide at a certain value of  $a$ . This happens for real (see [9]) as well as for complex (Fig. 2)  $\omega$ , but is symmetrically only for real  $\omega$ . At these points, the

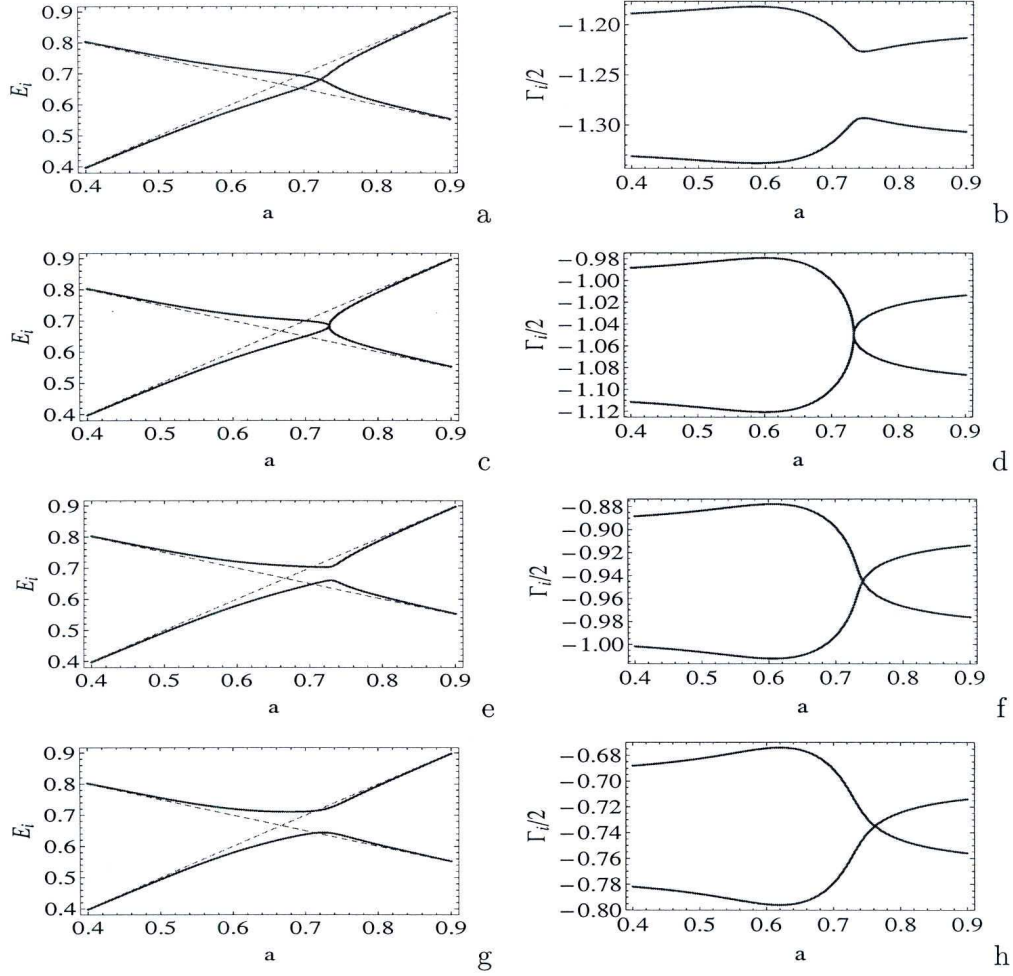


FIG. 1: Energies  $E_i$  and widths  $\Gamma_i/2$  (full lines) of  $N = 2$  states beyond (a,b), at (c,d) and below (e to h) the exceptional point. The parameters of the subfigures are  $\gamma_1/2 = 1.2$  (a,b);  $\gamma_1/2 = 1.0$  (c,d);  $\gamma_1/2 = 0.9$  (e,f);  $\gamma_1/2 = 0.7$  (g,h). Further parameters:  $e_1 = 1 - a/2$ ;  $e_2 = a$ ;  $\gamma_2/2 = 1.1\gamma_1/2$ ;  $\omega = (1 + i) 0.05$ . The dashed lines show  $e_i(a)$ .

two states are exchanged.

In both cases  $\gamma_1/2 < \gamma_1^{\text{cr}}/2$  and  $\gamma_1/2 > \gamma_1^{\text{cr}}/2$ , the asymptotic values 1 and 0 are reached in a smaller parameter range when  $\omega$  is real than in the case with complex  $\omega$ . Within this parameter range the two eigenfunctions are mixed. The range of mixing shrinks to one point when the two states really cross (at the exceptional point). It is especially large when two discrete states (with  $\gamma_i = 0$ ) avoid crossing, as can be seen from Fig. 5 in [9] (where the

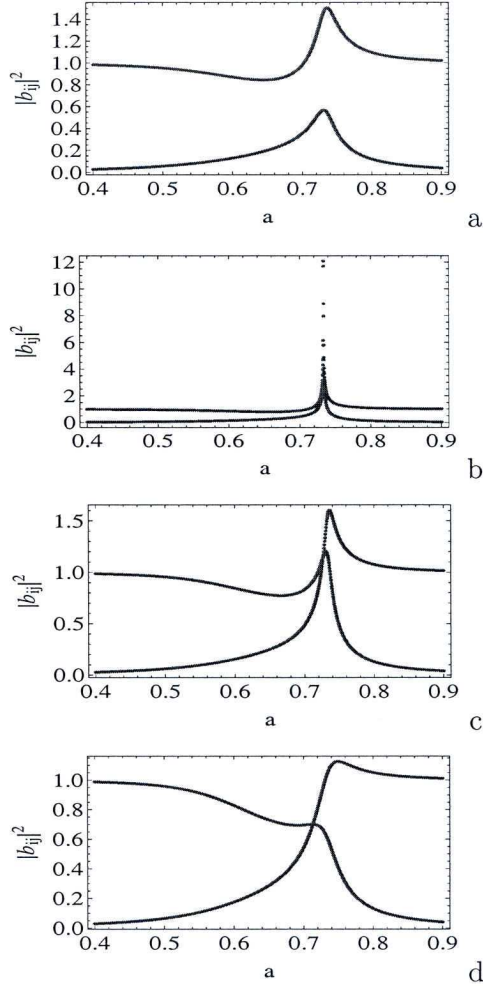


FIG. 2: The mixing coefficients  $|b_{ij}|^2$  of  $N = 2$  states beyond (a), at (b) and below (c,d) the exceptional point. The parameters are the same as in Fig. 1.

calculations are performed exactly with real  $\omega$  for all  $b_{ij}$ ).

The parameter range in which two states are mixed due to the existence of an exceptional point in the neighborhood plays an important role in realistic systems. It will be discussed in the following sections with more than one avoided crossing for both real and complex  $\omega$ .

#### IV. EIGENVALUES FOR $N = 4$ CROSSING LEVELS

Let us first compare the calculations with  $N = 2$  and  $N = 4$  states and imaginary coupling  $\omega = 0.05 i$  between discrete states and environment of scattering states (Fig. 3).

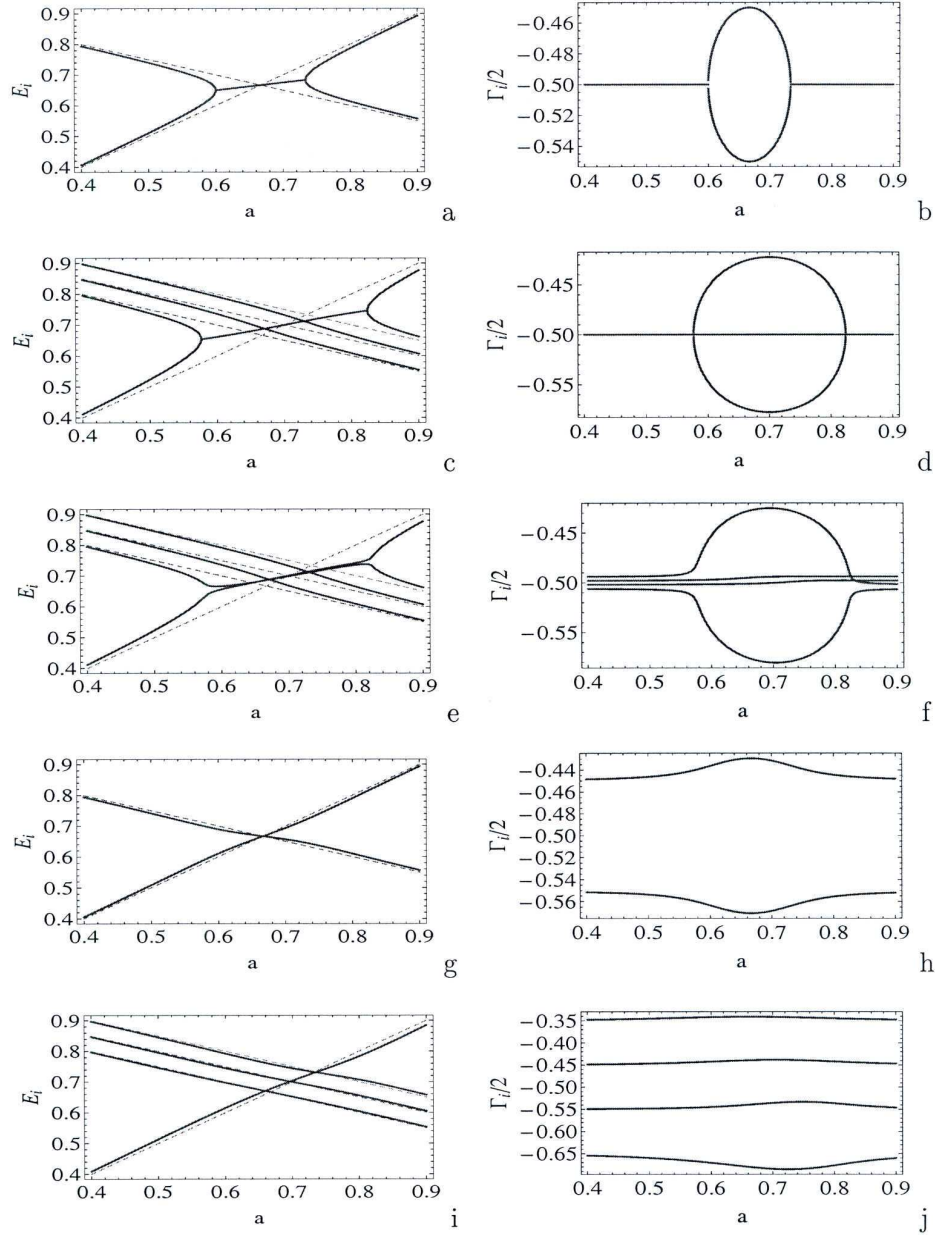


FIG. 3: Energies  $E_i$  and widths  $\Gamma_i/2$  (full lines) of  $N = 2$  states (a,b,g,h) and  $N = 4$  states (c to f and i, j) coupled to  $K = 1$  channel. The parameters of the subfigures are  $\gamma_i/2 = 0.5$  (a to d);  $\gamma_i/2 = 0.494, 0.498, 0.502, 0.506$  (e,f);  $\gamma_1/2 = 0.45, \gamma_2/2 = 0.55$  (g,h);  $\gamma_1/2 = 0.35; \gamma_2/2 = 0.45; \gamma_3/2 = 0.55; \gamma_4/2 = 0.65$  (i,j). Further parameters:  $N = 2$ :  $e_1 = 1 - a/2; e_2 = a$ ;  $N = 4$ :  $e_1 = 1 - a/2; e_2 = 1.05 - a/2; e_3 = 1.1 - a/2; e_4 = a; \omega = 0.05 i$ . The dashed lines show  $e_i(a)$ .

In the calculations, the eigenvalue trajectories  $E_i(a)$  and  $\Gamma_i(a)$  are traced as a function of the parameter  $a$  which is varied in such a manner that one state crosses in energy one and three, respectively, other states. The results show two exceptional points in both cases appearing at the two different parameter values  $a_1^{\text{cr}}$  and  $a_2^{\text{cr}}$ , see Figs. 3.a, b for two states and Figs.

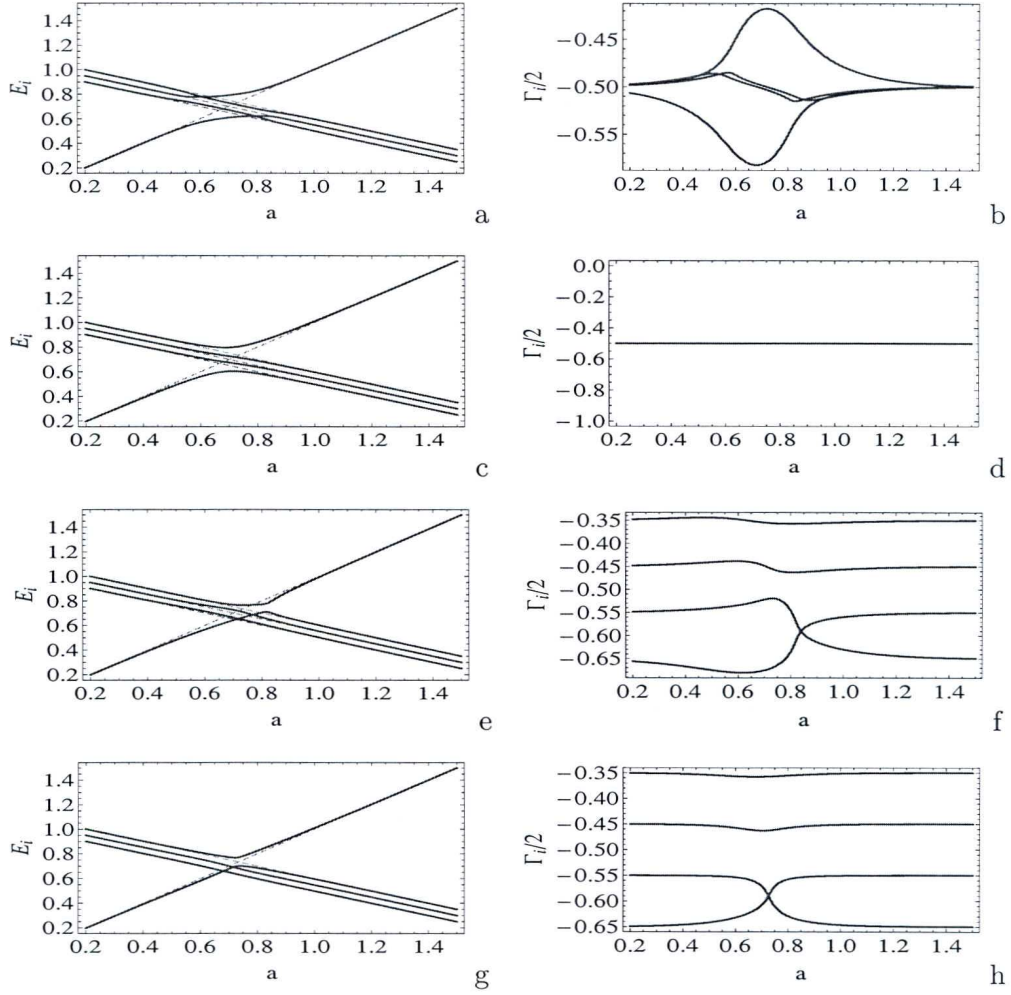


FIG. 4: The same as Fig. 3 but  $\omega = (1 + i) 0.05$  (a,b,e,f);  $\omega = 0.05$  (c,d,g,h);  $N = 4$ ;  $\gamma_i = 0.5$  (a to d);  $\gamma_i = 0.35; 0.45; 0.55; 0.65$  (e to h).

3.c to f for four states. In between these two values, the widths bifurcate: the differences  $\Delta\Gamma/2 \equiv |\Gamma_1/2 - \Gamma_2/2|$  blow up. The two-level case is described analytically by equations (10) to (16). The width bifurcation is completely reproduced in the numerical results.

The parameter range  $|a_1^{\text{cr}} - a_2^{\text{cr}}|$  is larger in the case with four states than in the other one due to the larger region in which avoided level crossings take place. Furthermore, the difference  $\Delta\Gamma/2$  is larger in the case of 4 states than in the case of 2 states. In the case that all states have equal widths  $\gamma_i/2$ , the widths  $\Gamma_i/2$  of only two states bifurcate also in the case with four states. The widths of the two other states remain unchanged (Figs. 3.c, d).

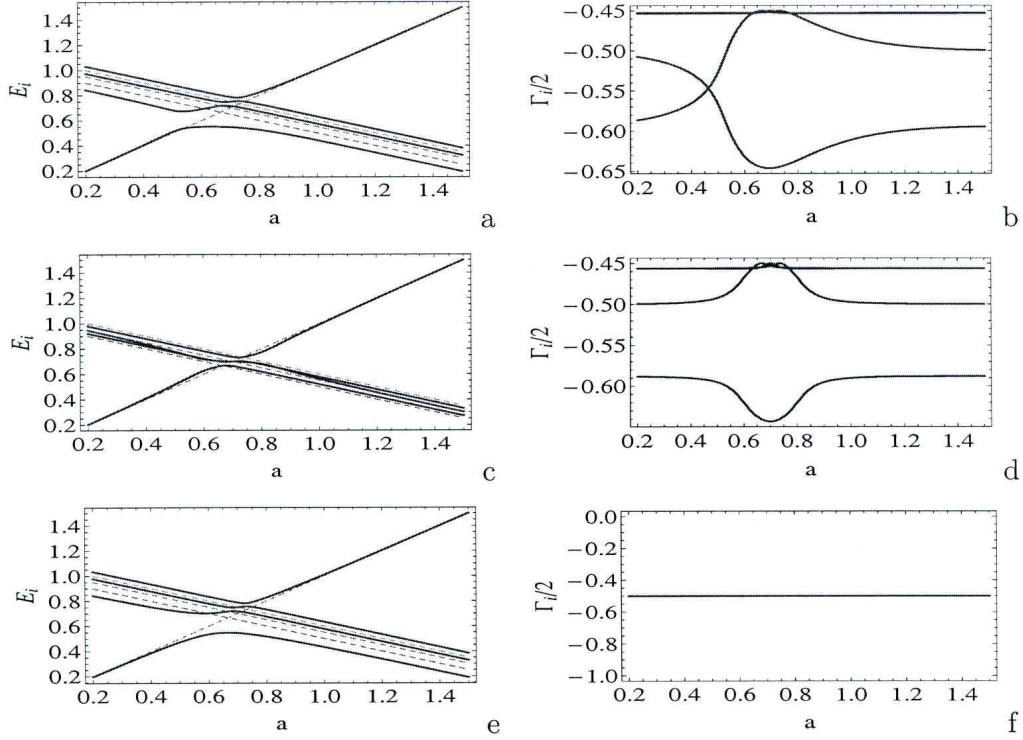


FIG. 5: The same as Fig. 3 but  $N = 4$  and  $K = 4$ ;  $\omega = (1 + i) 0.05$  (a,b);  $\omega = 0.05 i$  (c,d);  $\omega = 0.05$  (e,f);  $\gamma_i/2 = 0.5$ .

This result holds also when the different  $\gamma_i/2$  differ slightly from one another (Figs. 3.e, f). In this latter case, the two states avoid crossing at the two critical values  $a_1^{\text{cr}}$  and  $a_2^{\text{cr}}$  and the width bifurcation is almost the same as in the case with equal widths  $\gamma_i$ .

The situation changes completely when the widths  $\gamma_i$  differ stronger from one another. When  $|\gamma_i/2 - \gamma_{i\pm 1}/2| > |\epsilon_i - \epsilon_{i\pm 1}|$ , the states do not avoid crossing neither in the case with two states nor in the case with four states (Figs. 3.g to j). The eigenvalue trajectories cross freely in energy and the widths do (almost) not bifurcate. The dynamics of the system is therefore completely different from that determined by the results shown in Figs. 3.a to f.

In Fig. 4, we show the eigenvalues  $E_i$  and  $\Gamma_i/2$  for the case with four levels and one channel with complex and real coupling coefficients ( $\omega = 0.05 (1 + i)$  and  $\omega = 0.05$ , respectively). Width bifurcation can be seen when  $\omega$  is complex and the widths  $\gamma_i$  are equal (Figs. 4.a,

b), while the  $\Gamma_i = \gamma_i$  are independent of  $a$  when  $\omega$  is real (Figs. 4.c, d). The results with different  $\gamma_i$  differ from those obtained with imaginary coupling  $\omega = 0.05 i$  (Figs. 3.g to j): the widths of two states cross at parameter values at which their energies avoid crossing (Figs. 4.e to h).

In Fig. 5, we show the results of calculations with equal number of states and channels,  $N = 4$  and  $K = 4$ . Although usually  $K < N$  in realistic systems, the results allow us to receive a deeper understanding for the spectroscopic redistribution processes taking place in the critical region. The calculations are performed with the same parametric dependence of the energies as in the foregoing calculations with  $N = 4$  and  $K = 1$ . Further assumptions:  $\gamma_i = 0.5$  and  $\omega = 0.05 (1 + i)$ ,  $0.05 i$ , and  $0.05$ , respectively.

The results show width bifurcation when  $\omega$  is complex or imaginary (Figs. 5.a to d) which is however smaller than in the corresponding cases with  $K = 1$  (Figs. 4.a, b and Figs. 3.c, d, respectively). Instead, the widths  $\Gamma_i$  of the states are changed asymptotically due to the coupling to the different channels. When  $\omega$  is real (Figs. 5.e,f), the widths  $\Gamma_i/2$  are independent of  $a$  and are equal to  $\gamma_i/2 = 0.05$  ( $i = 1$  to  $4$ ).

## V. EIGENFUNCTIONS FOR $N = 4$ CROSSING LEVELS

The coefficients  $b_{ij}$  defined in (17) determine the mixing of the eigenfunctions  $\Phi_i$  in relation to the basic wavefunctions  $\phi_j$ . The mixing is nonvanishing in the neighborhood of the critical points of avoided level crossings as has been shown in exact numerical calculations for two crossing states and real coupling coefficients  $\omega_{ij}$  [9]. In the calculations of the present paper, the mixing of the wavefunctions is simulated by assuming a Gaussian distribution for the  $\omega_{ij}$ , equation (18). It reproduces very well the exact results obtained in [9].

In the following, we consider the mixing coefficients  $b_{ij}$  for all wavefunctions  $\Phi_i$  the eigenvalue trajectories of which are studied in Figs. 3 to 5 as a function of the parameter  $a$ . In Fig. 6, the coefficients  $|b_{ij}|^2$  are shown for two and four states with imaginary coupling  $\omega = 0.05 i$  (see the corresponding eigenvalue trajectories in Fig. 3). When the widths  $\gamma_i$  of all states are equal (Figs. 6.a, b),  $|b_{ij}|^2 \rightarrow \infty$  at the two exceptional points  $a_1^{\text{cr}}$  and  $a_2^{\text{cr}}$ . In the parameter range  $a_1^{\text{cr}} < a < a_2^{\text{cr}}$ , the wavefunctions are mixed while  $b_{ii} \rightarrow 1$  and  $b_{ij} \rightarrow 0$  for  $i \neq j$  beyond the two values  $a_{1,2}^{\text{cr}}$ . The states are completely (1:1) mixed in the range  $a_1^{\text{cr}} < a < a_2^{\text{cr}}$  in the two-level-case (Fig. 6.a). The picture is more complicated in the four-



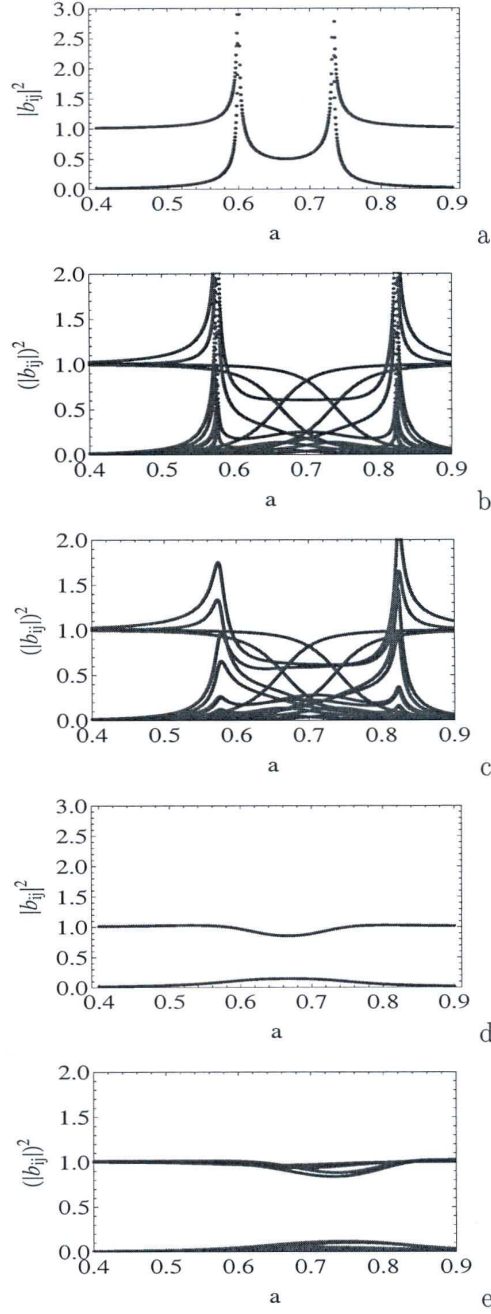


FIG. 6: The mixing coefficients  $|b_{ij}|^2$  of  $N = 2$  and  $N = 4$  states the eigenvalues of which are shown in Fig. 3;  $K = 1$  channel;  $\omega = 0.05 i$ .

level-case (Fig. 6.b). Here, all states are involved in the redistribution taking place in the critical parameter range  $a_1^{\text{cr}} < a < a_2^{\text{cr}}$ . The exchange of the two states the widths of which remain unchanged according to Fig. 3.d can be seen from the energy eigenvalue trajectories, Fig. 3.c, as well from the mixing coefficients, Fig. 6.b.

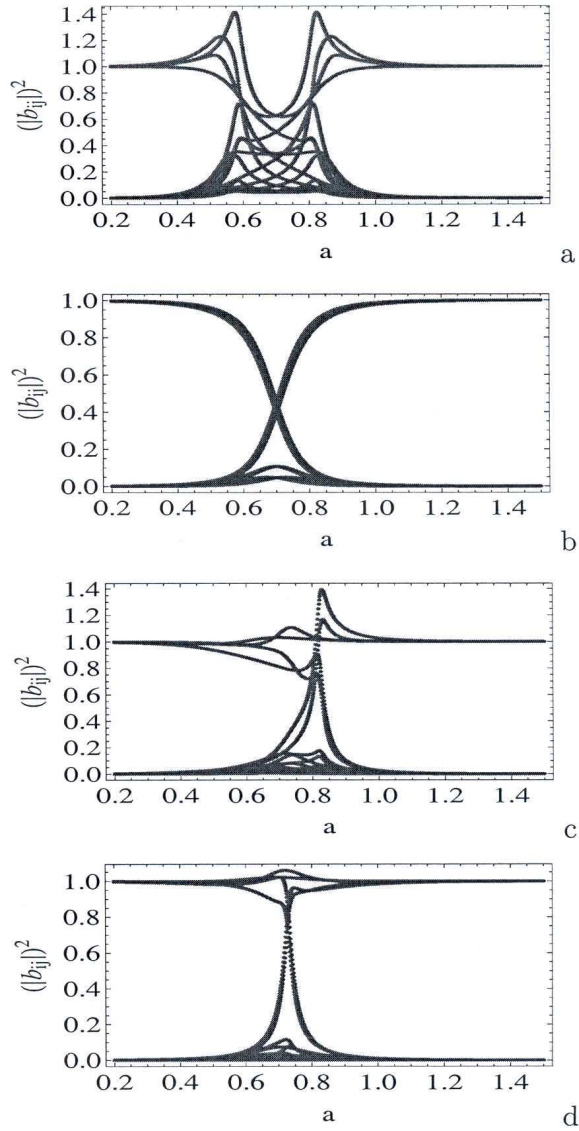


FIG. 7: The mixing coefficients  $|b_{ij}|^2$  of  $N = 4$  states the eigenvalues of which are shown in Fig. 4;  $K = 1$  channel;  $\omega = (1 + i) 0.05$  (a,c);  $\omega = 0.05$  (b,d).

The figures are similar when the widths  $\gamma_i$  of the states differ slightly from one another. Instead of exceptional points, there are avoided level crossings at  $a_1^{\text{cr}}$  and  $a_2^{\text{cr}}$ , see Fig. 6.c for the four-level-case. The mixing coefficients show a dependence on  $a$  which is similar to that obtained for equal widths (Fig. 6.b).

When the widths  $\gamma_i$  of the states  $i$  differ stronger from one another than in Fig. 6.c, the eigenfunctions remain almost unmixed for all parameter values  $a$  (Figs. 6.d, e). This result

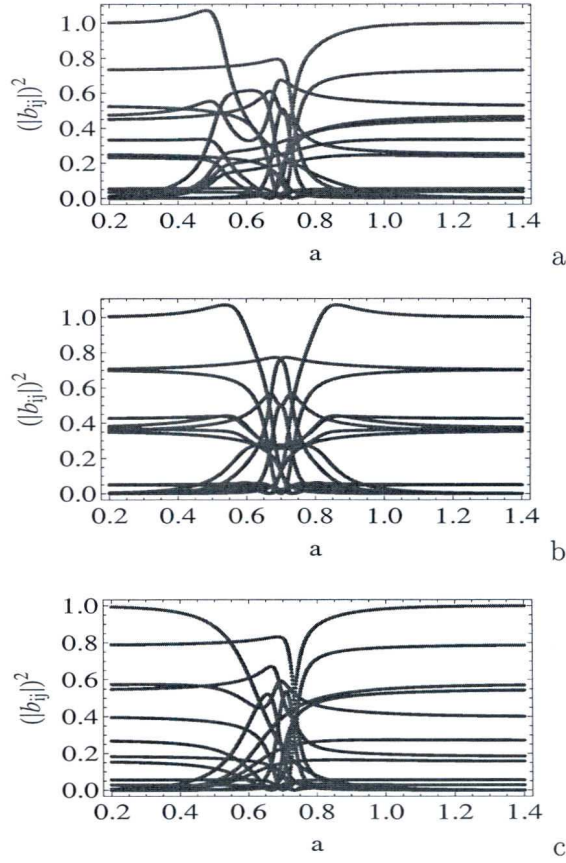


FIG. 8: The mixing coefficients  $|b_{ij}|^2$  of  $N = 4$  states the eigenvalues of which are shown in Fig. 5;  $K = 4$  channels;  $\omega = (1 + i) 0.05$  (a);  $\omega = 0.05 i$  (b);  $\omega = 0.05$  (c).

corresponds to the almost constant width trajectories  $\Gamma_i$  as a function of  $a$  (Figs. 3.h, j). An exchange of states does not take place (Figs. 3.g, i). These results show the great influence of the exceptional points onto the dynamics of the system considered.

The calculations in Figs. 3 and 6 are performed with imaginary coupling  $\omega = 0.05 i$ . For comparison, we show in Fig. 7 the mixing coefficients  $|b_{ij}|^2$  when  $\omega$  is complex and real, respectively, for the four-level-case (corresponding to the eigenvalue trajectories in Fig. 4). When all  $\gamma_i$  are equal to one another and  $\omega$  is complex, the mixing coefficients  $|b_{ij}|^2$  point to the participation of all states in the redistribution process in the critical parameter range (Fig. 7.a). This corresponds fully to the corresponding eigenvalue trajectories that show level exchange as well as width bifurcation (Figs. 4.a,b). When the coupling is real,

however, the wavefunctions of only two states are mixed while the wavefunctions of the other two states remain almost unchanged in the critical region (Fig. 7.b).

The mixing of the eigenfunctions is completely different from that discussed above when the widths  $\gamma_i$  differ more strongly from one another. A mixing of the wavefunctions appears only when the energy trajectories  $E_i(a)$  avoid crossing and the width trajectories  $\Gamma_i(a)$  cross, compare Figs. 4.e to h with the corresponding Figs. 7.c, d. A width bifurcation does not take place.

The mixing coefficients  $|b_{ij}|^2$  for the case with  $N = 4$  states coupled to  $K = 4$  channels are shown in Fig. 8 (parameters the same as in Fig. 5). The differences between the cases with coupling to 4 channels to those with coupling to only 1 channel can be seen by comparing Fig. 8.a with Fig. 7.a, Fig. 8.b with 6.b and Fig. 8.c with Fig. 7.b. The mixing of the wavefunctions by coupling the system to four channels is more complicated than that by coupling to only one channel. This statement holds true also when  $\omega$  is imaginary. Furthermore, an additional mixing is caused by the avoided level crossing at small  $a$  in the four-channel-case when  $\omega$  is complex.

## VI. EIGENVALUES FOR $N = 10$ CROSSING LEVELS

We continue our studies with the matrix (6) by choosing  $N = 10$  states coupled to 1 channel. The eigenvalue trajectories  $E_i(a)$  and  $\Gamma_i(a)$  are shown in Figs. 9 and 10. In these cases, one of the states crosses in energy the remaining nine states one by one. The nine states have the same parametric energy dependence of  $a$  and are shifted equidistantly relative to one another.

In Fig. 9.a, b we show the results obtained with  $\omega = 0.07 i$  and  $\gamma_i = 0.5$  for all states. The results are similar to those for the 4-level case (Figs. 3.c, d). Two exceptional points appear as well as width bifurcation: the width of one of the states is much larger while that of another one is much smaller than the widths of all the other states in the whole critical parameter range between the two exceptional points.

In Figs. 9.c to f, the widths  $\gamma_i$  differ from one another. We compare the results obtained with an imaginary and with a real coupling constant,  $\omega = 0.07 i$  and 0.07, respectively. When  $\omega$  is real (Figs. 9.e, f), the energy trajectories  $E_i(a)$  are very regular: avoided level crossings appear one by one with all nine states. An exceptional point can be found only by

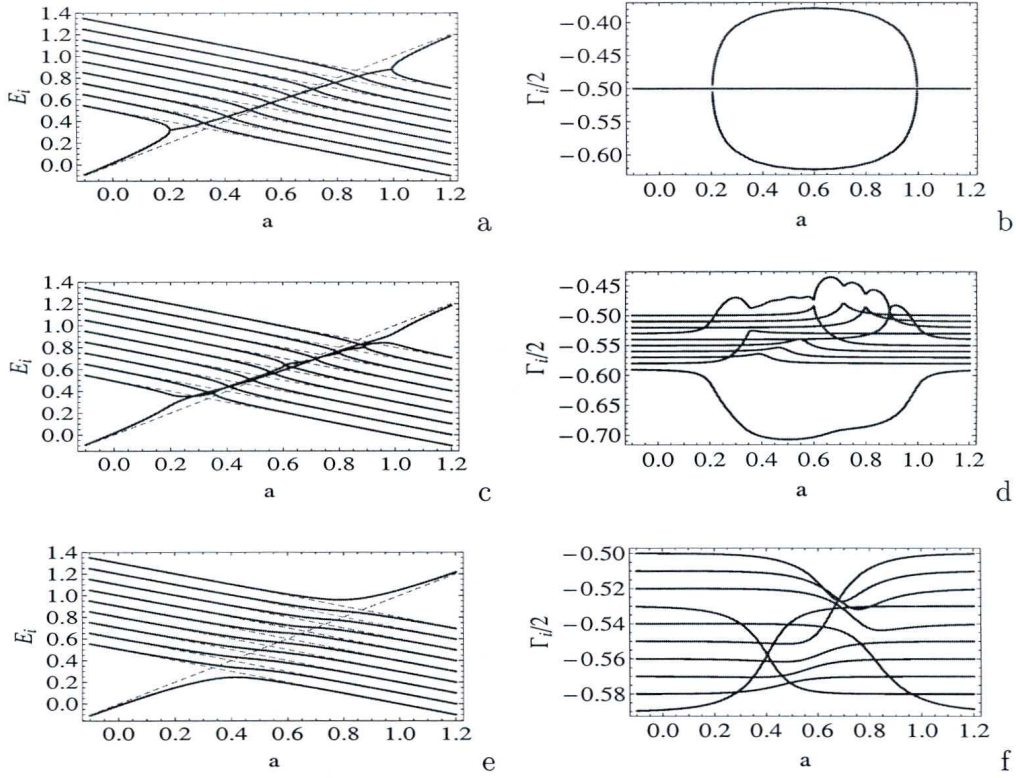


FIG. 9: Energies  $E_i$  and widths  $\Gamma_i/2$  (full lines) of  $N = 10$  states coupled to  $K = 1$  channel. The parameters of the subfigures are  $\gamma_i/2 = 0.5$  (a,b);  $\gamma_i/2 = 0.50; 0.51; 0.52; 0.53; 0.54; 0.55; 0.56; 0.57; 0.58; 0.59$  (c to f);  $\omega = 0.07 i$  (a to d);  $0.07$  (e,f). Further parameters:  $e_i = 1 - a/2; 1.1 - a/2; 1.2 - a/2; 1.3 - a/2; 0.9 - a/2; 0.8 - a/2; 0.7 - a/2; 0.6 - a/2; 0.5 - a/2; a$ . The dashed lines show  $e_i(a)$ .

analytical continuation into the continuum (see [8]). The width trajectories  $\Gamma_i(a)$  are less regular: they cross at several parameter values  $a$ . According to the results obtained for a smaller number of states in sections III to V, the widths do not bifurcate when  $\omega$  is real.

When  $\omega$  is imaginary, the energy trajectories  $E_i(a)$  are also regular (Fig. 9.c). Fig. 9.d shows nicely how widths continue to bifurcate such that the broad state remains broad and the narrow state remains narrow for all  $a$  in the critical region. Mostly, the widths of two states are different from one another when the energy trajectories cross. The states can, nevertheless, be exchanged as can be seen from Fig. 9.c.

In Fig. 10, we show results obtained with the imaginary coupling constant  $\omega = 0.05 i$  (being smaller than in Figs. 9.c, d) as well as those obtained with the larger values  $\omega =$

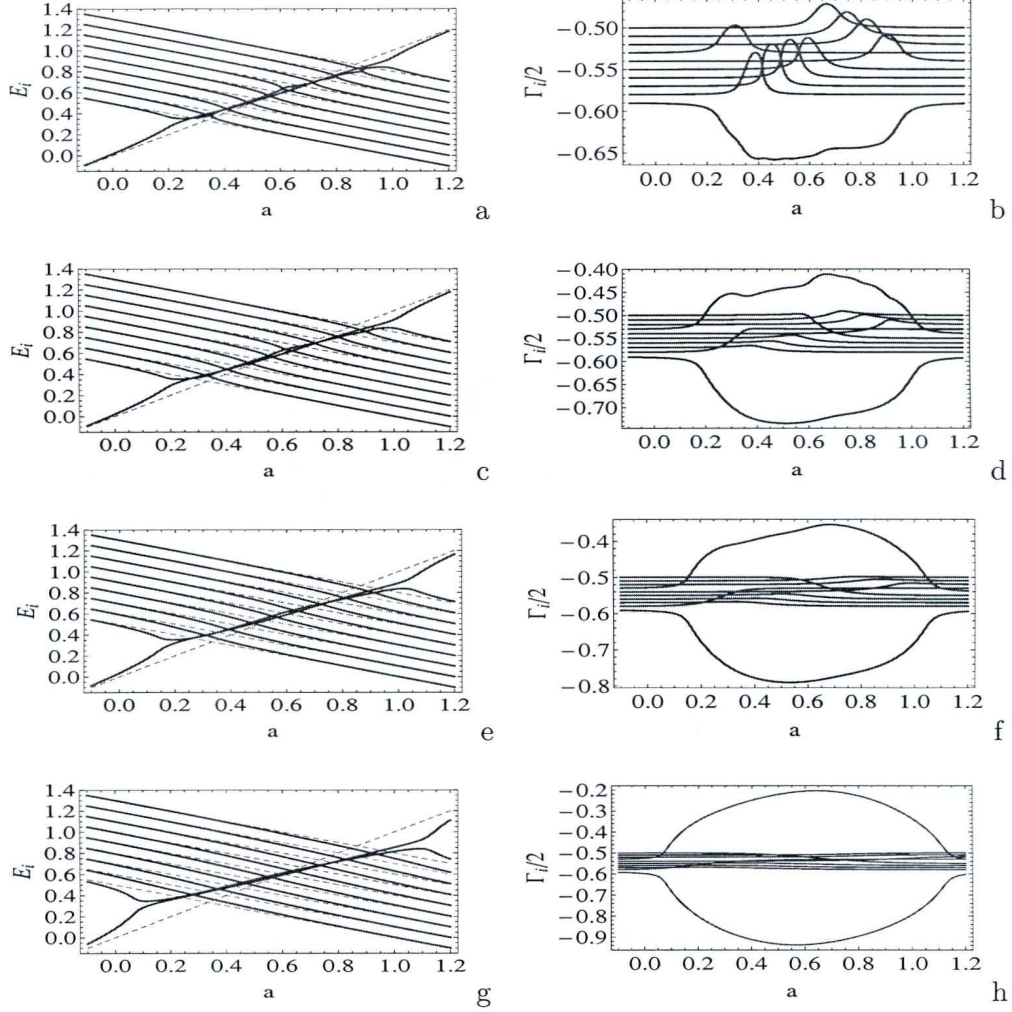


FIG. 10: The same as Fig. 9 but  $\omega = 0.05 i$  (a,b);  $\omega = 0.08 i$  (c,d);  $\omega = 0.10 i$  (e,f);  $\omega = 0.15 i$  (g,h).

$0.08 i$ ,  $0.10 i$ ,  $0.15 i$  (Figs. 10.a,b and Figs. 10.c to h, respectively). We see width bifurcation similar as in Fig. 3.d for  $N = 4$  states and in Fig. 9.b for 10 states with equal widths  $\gamma_i$ . In any case, width bifurcation appears in the whole critical parameter range between the two exceptional points. The width bifurcation occurring in the case of 10 levels is stronger than that with a smaller number of levels (compare section IV). The 9 states crossed by the state 10 are exchanged in the critical parameter region as can be seen from the corresponding Figs. 10.a, c, e, g.

The results shown in Figs. 9 and 10 follow from calculations with a toy model being symmetrical in relation to the crossing states. In the critical parameter range, the states



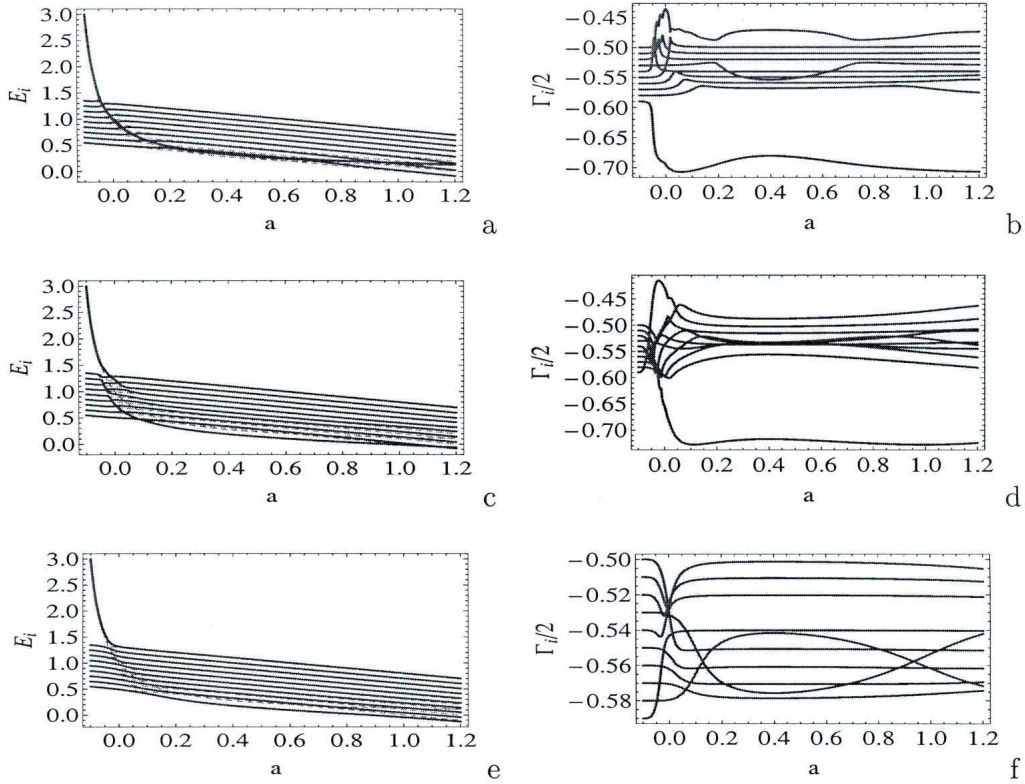


FIG. 11: The same as Fig. 9 but  $e_{10} = 0.15/(0.15 + a)$ ;  $\omega = 0.07 i$  (a, b);  $\omega = (1 + i) 0.07$  (c, d) and  $\omega = 0.07$  (e,f).

are exchanged in all cases but 8 of them do not contribute actively to the width bifurcation when  $\omega$  is imaginary. This result follows from the high symmetry of the exceptional points in relation to the crossing states, i.e. from the linear dependence of the energy of the crossing state on the parameter  $a$ ,  $e_{10}(a) = a$ . The 8 states play the role of 'observers' similarly as discussed in a toy model with 4 states [17] and in a realistic model with 3 states [22].

In order to exclude the high symmetry of the exceptional points in relation to nearby states we show in Fig. 11 the results of another version of the toy model. Instead of  $e_{10}(a) = a$  in Figs. 9 and 10, we use  $e_{10} = 0.15/(0.15 + a)$  in Fig. 11. The width  $\Gamma_i$  of one of the states becomes large in the critical parameter range when  $\omega$  is imaginary or complex (Figs. 11.b and d, respectively), while the widths of all the other states are much smaller. This result reflects the situation observed in many realistic cases (see e.g. the review [8] and also [23]). A separation of a short-lived state from the other ones does not appear when  $\omega$

is real (Fig. 11.f).

## VII. DISCUSSION OF THE RESULTS

In sections III to VI, we showed results obtained numerically for the eigenvalues  $\mathcal{E}_i = E_i - i/2 \Gamma_i$  and eigenfunctions  $\Phi_i$  by using the matrix (5) (or (6)) with 2, 4 and 10 levels, respectively. Only the energies  $e_i$  of the states are varied as a function of a certain parameter  $a$ . The widths  $\gamma_i$  are assumed to be constant, the interaction  $\omega_{ij}$  between the levels  $i$  and  $j$  is either zero or simulated by the Gaussian distribution (18) where  $\omega$  is the same for all states (and also independent of  $a$ ), and the self-energy terms are considered to be included into the diagonal matrix elements. Most interesting is the one-channel case for different  $N$ , e.g. the matrix (6) for  $N = 4$ .

This toy model describes well the generic features of open quantum systems. The  $\omega_{ij}$  are complex. They stand for the interaction of the states via the environment (continuum of scattering wavefunctions):  $\text{Re}(\omega_{ij})$  arises from the principal value integral (3) and  $\text{Im}(\omega_{ij})$  is the residuum (4). Both parts play an important role for the dynamics of the open quantum system at high level density where the resonance states overlap. The influence of  $\text{Re}(\omega_{ij})$  onto eigenvalues  $\mathcal{E}_i$  and eigenfunctions  $\Phi_i$  is studied numerically exact for  $N = 2$  levels in an earlier paper [9]. It causes the avoided crossing of the states which is well known for discrete as well as for narrow resonance states.

Equations (13) to (16) show analytically the main difference between  $\text{Re}(\omega_{ij})$  and  $\text{Im}(\omega_{ij})$  in the 2-level case when the widths of the two states are equal,  $\gamma_1 = \gamma_2$ . According to (13), an exceptional point can be found only by analytical continuation into the continuum when  $\omega_{ij}$  is real. Thus, the two states avoid crossing as it is very well known for discrete as well as for narrow resonance states [9]. In contrast,  $\text{Im}(\omega_{ij})$  causes two exceptional points according to equation (14). Most interesting is the width bifurcation arising in between the two exceptional points according to (16).

The analytical results (13) to (16) are well reproduced in our numerical calculations for the eigenvalues  $\mathcal{E}_i$ , Figs. 3.a, b. Also the eigenfunctions  $\Phi_i$  show the two exceptional points:  $|b_{ij}|^2 \rightarrow \infty$  in approaching them, Fig. 6.a. In between the two exceptional points, the wavefunctions of the two states are strongly mixed. The mixing is 1:1 in the middle between the two singular points. Beyond the critical region between the two exceptional points, the



$|b_{ij}|^2$  approach 1 when  $i = j$  and 0 when  $i \neq j$ . Here, the two states may be exchanged, at most. The figures 3.a,b and 6.a represent the basic process of width bifurcation according to the analytical expressions (15) and (16).

In sections IV, V and VI of the present paper, numerical results for 4 and 10 states are shown under similar conditions, i.e. with equal or nearly equal  $\gamma_i$  for all states: Figs. 3.c to f and Figs. 6.b and c for the eigenvalues and eigenfunctions, respectively, of 4 states, and Figs. 9.a, b for the eigenvalues of 10 states. The development of width bifurcation as a function of increasing imaginary coupling vector  $\omega$  can be seen in Fig. 10 for  $N = 10$  states when the single widths  $\gamma_i$  are different from one another. The uniform width bifurcation in Fig. 9.b appears at a smaller value of  $\text{Im}(\omega)$  than in Fig. 10.h due to the different values of the single  $\gamma_i$  in the last case. Generally, the width bifurcation is stronger when the number of states is larger.

The influence of  $\text{Re}(\omega_{ij})$  onto the eigenvalue trajectories and eigenfunctions is also shown for  $N = 4$  and 10 (Figs. 4.c, d for the eigenvalues of 4 states, Fig. 7.b for the eigenfunctions of 4 states and Figs. 9.e, f for the eigenvalues of 10 states). Under the influence of  $\text{Re}(\omega_{ij})$ , the states avoid crossing in energy and the widths do not bifurcate. When the calculation is performed with complex coupling vector ( $\text{Re}(\omega_{ij} \neq 0)$  and  $\text{Im}(\omega_{ij} \neq 0)$ ), the widths bifurcate with some shift of the position of the maximum relative to that of the minimum (Figs. 4.a, b) and a larger parameter range of mixed wavefunctions (Fig. 7.a).

According to the results presented in sections IV to VI the eigenvalue trajectories are strongly influenced by the values of the external (fixed) parameters when the resonances overlap and exceptional points determine the dynamics of the system. However, the eigenvalue trajectories are almost independent of one another when the degree of resonance overlapping is small. Examples are Figs. 3.g to j and 4.e to h for the eigenvalues of, respectively, two and four resonance states and the corresponding Figs. 6.d,e and 7.c,d for the eigenfunctions of these states. These results show the strong influence of external parameters onto the dynamics of the system at high level density which is known from the study of realistic cases. An example is the enhanced transmission through microwave cavities when the formation of whispering gallery modes is supported by the manner the leads are attached to the cavity [24].

Width bifurcation is directly related to the *alignment* of one of the  $N$  resonance states of the open quantum system to a decay channel ( $K = 1$ ) with the consequence that it becomes

short-lived while other states become *trapped* (long-lived), i.e. more or less decoupled from the environment. Mathematically, the alignment of a resonance state is possible since the eigenfunctions of a non-Hermitian operator are biorthogonal and their phases (relative to those of the eigenfunctions of the other states) are not rigid in approaching an exceptional point, see equation (12). Width bifurcation appears therefore in our calculations when  $K = 1$  and  $N = 4$  or  $10$ . This corresponds to realistic situations in which usually  $K < N$ . Width bifurcation does, however, not appear when  $N = 4$  states are coupled to  $K = 4$  channels (Fig. 5) although the wavefunctions are strongly mixed in the critical parameter region also in this case (Fig. 8).

An artifact of our model calculations is the assumption of equidistant energies  $e_i$  of all but one state which are crossed by one state the energy of which depends linearly on the parameter  $a$ . Thus, the critical points are symmetrically in relation to the two neighboring states, and  $N - 2$  states do not contribute actively to the width bifurcation taking place in the whole system. In Fig. 11, we show results obtained when the symmetry is somewhat disturbed (as it is usually the case in realistic systems). In such a case, the width of one state separates from those of *all* the other states. That means, all nine states remain trapped (decoupled) in the whole critical parameter range. This result corresponds to results obtained theoretically as well as experimentally in different realistic systems (see section 4 in the review [8]).

It should be added here, that asymptotically (beyond the critical parameter region) the states can be exchanged at most. This is the case, indeed, in all our calculations. All redistribution processes caused by the exceptional points take place only in the critical parameter region. This holds true for real as well as for imaginary coupling coefficients  $\omega_{ij}$  and can be seen also in the mixing coefficients  $b_{ij}$  which approach 1 or 0 when  $i = j$  and  $i \neq j$ , respectively, beyond the critical parameter region. The two cases with real and imaginary  $\omega$  differ, however, by the length of the critical region.

## VIII. CONCLUSIONS

The results of the present paper show that exceptional points cause width bifurcation because the coupling of the states via the environment (continuum of scattering wavefunctions) is complex. An example are the bound states in the continuum appearing at a *finite*

value of the coupling strength between system and environment when the interplay between internal and external interaction is taken into account, see section 4.4 of the review [8]. Of particular interest is the width bifurcation appearing at high level density. Here, many exceptional points are near to one another. As shown in the present paper, width bifurcation causes, under this condition, a splitting of the system into two parts one of which exists in the short-time scale while the other one appears in the long-time scale. The two parts can not be observed together. The long-lived states occur as fluctuations in the short-time scale while the short-lived states perform a smooth background in the long-time scale.

This phenomenon is known in literature from theoretical as well as experimental studies on different small quantum systems and systems equivalent to them (see examples in the review [8] and in [17, 25, 26]). In many-body open quantum systems, it is called mostly *dynamical phase transition*. It is known also in optics where it is called *superradiant phase transition* according to Dicke [14]. In PT-symmetric systems, the phase transition is called mostly *PT-symmetry breaking* [27].

Common to all these studies is that the dynamical phase transition is very robust when the necessary conditions are fulfilled, i.e. when the level density is high and the dynamics of the system is determined by exceptional points. Although the existence of exceptional points is decisive (as shown in the present paper), the dynamical phase transition does *not* appear at the parameter value which gives the position of the exceptional point itself. Instead, the phase transition occurs in the neighborhood of one (or several) exceptional points. Such a result is known from different experimental studies on concrete realistic systems. It is discussed in e.g. [28]. The results of the present paper show that the critical parameter range is determined by the distance between (at least) two exceptional points.

The dynamical phase transition appearing in small quantum systems at high level density, causes a new understanding of time as discussed in [11]. Time which is characteristic of the system, is inverse proportional to the widths  $\Gamma_i$  and related therefore directly to the non-Hermitian part of the Hamilton operator. The widths do not increase limitless as shown in the present paper. Instead, the system is dynamically stabilized: the lifetimes of the states of the system are increased and the system as a whole is stabilized by ejecting the short-lived state from the system at the dynamical phase transition. Thus, the time characteristic of the system is bounded from below in a similar manner as the energy. Beyond the dynamical phase transition, all states have lost their original spectroscopic features and the number of

states is reduced.

This fact is very well known in nuclear physics (although very seldom interpreted in this manner). The properties of compound nuclei are described well by the *Unified theory of nuclear reactions* developed by Feshbach [7], which contains both the short-lived direct reaction part and the long-lived compound nuclear reaction part. However, Feshbach introduces statistical assumptions in order to describe the long-lived compound nuclear states. This is in contrast to the calculations in the present paper where the long-lived states are described *without* any statistical assumptions. Instead the long-lived states are shown by us to arise from width bifurcation causing a dynamical stabilization of the system at high level density, a phenomenon that is caused by exceptional points.

Many of these results seem to be counterintuitive. They allow us, however, to explain some unexpected experimental results. For example, the crossover from the mesoscopic to a universal phase for transmission in quantum dots observed experimentally [3] can be explained qualitatively by the formation of the short-lived resonance state at the dynamical phase transition. The results of the present paper support this interpretation [12] of the experimental results. Another example is the experimental observation [6] of non-statistical effects in nuclear reactions on middle-heavy nuclei. The data show directly the formation of different time scales in the system at high level density. Other examples are discussed in [8, 11, 28].

The long-lived states beyond the dynamical phase transition are strongly mixed and show chaotic features. The random matrix theory is surely applicable only after averaging over different decay channels (as usually done), i.e. it is not applicable to the description of small systems coupled to one channel (and, respectively, to two channels in the case of transmission through the system). A theoretical analysis of the spectra (without any statistical assumptions) by restricting to the results obtained from one decay channel according to the recent experimental data on compound nuclei [5] is not performed up to now. On the basis of the results of the present paper, it can be stated today only the following. The mixing of the long-lived states (beyond the dynamical phase transition) is caused by complex many-body forces via the continuum of scattering wavefunctions (simulated by the  $\omega_{ij}$  in our calculations) and not by two-body forces. This may provide an explanation of the fact why compound nucleus spectra (after averaging over different channels and beyond decay thresholds) may be described by a Gaussian orthogonal ensemble (containing many-body

forces), but not by a two-body random ensemble. This point should be studied in future in more detail.

In order to prove the role of exceptional points in an open many-level quantum system it is highly interesting to study experimentally time symmetry breaking caused by the influence of a nearby state onto an exceptional point. Theoretical studies with a symmetrical influence (as in most calculations of the present paper) can surely not describe the properties of realistic systems with broken time symmetry. Symmetry breaking influences not only width bifurcation (as shown in Fig. 11) but will prove, above all, the irreversible processes caused by exceptional points in open quantum systems. These processes are decisive, among others, for the dynamical stabilization of quantum systems and the formation of quantum chaos.

Finally we remark that the sensitive dependence of the dynamics of an open quantum system on the value of external parameters (as shown in the present paper) can be used in order to construct small systems with desired properties. This point is important for applications.

\* email: eleuchh@iro.umontreal.ca

\*\* email: rotter@pks.mpg.de

- 
- [1] A.M. Lane and R.G. Thomas, *Rev. Mod. Phys.* **30**, 257 (1958); P. Descouvemont and D. Baye, *Rep. Prog. Phys.* **73**, 036301 (2010)
  - [2] C. Mahaux and H.A. Weidenmüller, *Shell model approach to nuclear reactions*, Springer 1969
  - [3] A. Yacoby, M. Heiblum, D. Mahalu, and H. Shtrikman, *Phys. Rev. Lett.* **20**, 4047 (1995); R. Schuster, E. Buks, M. Heiblum, D. Mahalu, V. Umansky, and H. Shtrikman, *Nature* **385**, 417 (1997); M. Avinun-Kalish, M. Heiblum, O. Zarchin, D. Mahalu, and V. Umansky, *Nature* **436**, 529 (2005)
  - [4] M. Goldstein and R. Berkovits, *New J. Phys.* **9**, 118 (2007); D.I. Golosov, and Y. Gefen, *New J. Phys.* **9**, 120 (2007); Y. Oreg, *New J. Phys.* **9**, 122 (2007); P.G. Silvestrov and Y. Imry, *New J. Phys.* **9**, 125 (2007)
  - [5] P.E. Koehler, F. Becvar, M. Krticka, J.A. Harvey, and K.H. Guber, *Phys. Rev. Lett.* **105**,

- 072502 (2010); P.E. Koehler, Phys. Rev. C **84**, 034312 (2011)
- [6] E.P. Kanter, D. Kollewe, K. Komaki, I. Leuca, G.M. Temmer, and W.M. Gibson, Nucl. Phys. A **299**, 230 (1978)
- [7] H. Feshbach, Ann. Phys. (N.Y.) **5**, 357 (1958) and **19**, 287 (1962)
- [8] I. Rotter, J. Phys. A **42**, 153001 (2009)
- [9] I. Rotter, Phys. Rev. E **64**, 036213 (2001)
- [10] P. Kleinwächter and I. Rotter, Phys. Rev. C **32**, 1742 (1985)
- [11] I. Rotter, Contribution to the Special Issue *Quantum Physics with Non-Hermitian Operators: Theory and Experiment*, Fortschritte der Physik - Progress of Physics **61**, 178 (2013); DOI: 10.1002/prop.201200054
- [12] M. Müller and I. Rotter, Phys. Rev. A **80**, 042705 (2009)
- [13] G.A. Álvarez, E.P. Danieli, P.R. Levstein, and H.M. Pastawski, J. Chem. Phys. **124**, 194507 (2006); G.A. Álvarez, E.P. Danieli, P.R. Levstein, and H.M. Pastawski, Phys. Rev. A **75**, 062116 (2007); H.M. Pastawski, Physica B **398**, 278 (2007)
- [14] R.H. Dicke, Phys. Rev. **93**, 99 (1954)
- [15] V.V. Sokolov and V.G. Zelevinsky, Ann. Phys. (NY) **216**, 323 (1992)
- [16] Y. Yoon, L. Mourokh, T. Morimoto, N. Aoki, Y. Ochiai, J.L. Reno, and J.P. Bird, Phys. Rev. Lett. **99**, 136805 (2007); Y. Yoon, M.G. Kang, T. Morimoto, L. Mourokh, N. Aoki, J.L. Reno, J.P. Bird, and Y. Ochiai, Phys. Rev. B **79**, 121304(R) (2009); Y. Yoon, M.G. Kang, T. Morimoto, M. Kida, N. Aoki, J.L. Reno, Y. Ochiai, L. Mourokh, J. Fransson, and J.P. Bird, Phys. Rev. X **2**, 021003 (2012)
- [17] H. Eleuch and I. Rotter, Contribution to the Special Issue *Quantum Physics with Non-Hermitian Operators: Theory and Experiment*, Fortschritte der Physik - Progress of Physics **61**, 194 (2013); DOI: 10.1002/prop.201200062
- [18] T. Bienaimé, N. Piovella, and R. Kaiser, arXiv:1201.2274 (2012)
- [19] C. Jung, M. Müller, and I. Rotter, Phys. Rev. E **60**, 114 (1999)
- [20] T. Kato, *Perturbation Theory for Linear Operators* Springer, Berlin, 1966
- [21] In studies by other researchers, the factor  $i$  in (11) does not appear. This difference is discussed in detail and compared with experimental data in the Appendix of [11] and in section 2.5 of [8].
- [22] I. Rotter and A.F. Sadreev, Phys. Rev. E **69**, 066201 (2004) and Phys. Rev. E **71**, 036227

(2005)

- [23] W. Iskra, I. Rotter, and F.M. Dittes, *Phys. Rev. C* **47**, 1086 (1993)
- [24] R.G. Nazmitdinov, K.N. Pichugin, I. Rotter, and P. Seba, *Phys. Rev. E* **64**, 056214 (2001)  
and *Phys. Rev. B* **66**, 085322 (2002)
- [25] I. Rotter, *EPJ Web of Conferences* **21**, 04002 (2012)
- [26] I. Rotter, *J. Modern Physics* **1**, 303 (2010)
- [27] A. Guo, G.J. Salamo, D. Duchesne, R. Morandotti, M. Volatier-Ravat, V. Aimez, G.A. Siviloglou, and D.N. Christodoulides, *Phys. Rev. Lett.* **103**, 093902 (2009); C.E. Rüter, K.G. Makris, R. El-Ganainy, D.N. Christodoulides, M. Segev, and D. Kip, *Nature Physics* **6**, 192 (2010); T. Kottos, *Nature Physics* **6**, 166 (2010)
- [28] I. Rotter, *J. Opt.* **12**, 065701 (2010)